Automatic Segmentation of the Inferior Vena Cava from M-mode Ultrasound Images

David Chaparro-Victoria[1], Amelia Campos-Saenz de Santamaría[2,3], Silvia Crespo-Aznarez[2,3], Laura Esterellas-Sánchez[2], Vanesa Garcés-Horna[2,3], Marta Sánchez-Marteles[2,3], Juan Pablo Martínez[4,3,5], Violeta Monasterio[1], Jorge Rubio-Gracia[2,3,6], Alejandro Alcaine[1]

[1] University San Jorge, Villanueva de Gállego (Zaragoza), Spain.
[2] Internal Medicine Department. Hospital Clínico Universitario "Lozano Blesa". Zaragoza. Spain
[3] Aragón Health Research Institute (IIS Aragón), Zaragoza, Spain.
[4] Aragón Institute of Engineering Research (I3A), University of Zaragoza, Zaragoza, Spain.
[5] CIBER in Bioengineering, Biomaterials and Nanomedicine (CIBER-BBN), Zaragoza, Spain.
[6] School of Medicine, University of Zaragoza, Zaragoza, Spain.

Abstract

Systemic venous congestion (SVC) is a critical factor in patients with heart and kidney failure, a condition known as cardiorenal syndrome (CRS). The Venous Excess Ultrasound grading System (VExUS) protocol represents a significant advance in the assessment of SVC using point-of-care ultrasound. The first step of this protocol consists of determining the maximum diameter of the inferior vena cava (IVC) in M-mode ultrasound images, a task currently performed manually. This work presents a method for the automatic segmentation and characterization of the IVC. The method was evaluated on a set of 20 images belonging to 13 patients with CRS. The maximum diameter determined automatically was compared with that measured during clinical practice. Results showed a mean error of -0.015 ± 0.318 *cm, with a Spearman correlation of* $\rho_s = 0.850$ *and a Lin coefficient of* $\rho_c = 0.864$*. Therefore, the proposed method achieves a reasonably accurate assessment of the maximum diameter of the IVC within the context of the VExUS protocol.*

1. Introduction

Cardiovascular diseases are the leading cause of death globally, accounting for 32% of global mortality [1]. Among these, heart failure (HF) is the most prevalent, representing the main cause of hospitalisation in people over 65 years old and the leading cause of admission to internal medicine services [2]. HF is a complex disease in which multiple pathophysiological pathways are activated as compensatory mechanisms for the cardiac dysfunction caused by multiple etiologies [3–5]. Systemic venous congestion (SVC) is a key element in the management of HF, given its demonstrated influence on both pathophysiology and prognosis, particularly in patients with coexisting HF and renal failure, a condition known as cardiorenal syndrome (CRS) [3, 6].

Patients with CRS present a significant challenge in cases where physical examination or conventional laboratory tests may not be sufficient for an accurate diagnosis and adapted treatment [7, 8]. Recently, Beaubien-Souligny W. *et al.* [9, 10] proposed a new point-of-care ultrasound protocol called Venous Excess Ultrasound Grading System (VExUS), aiming to improve the quantification of congestion in CRS patients, based on the analysis of the venous flow patterns observed by pulsed Doppler US imaging in three abdominal veins (suprahepatic, portal, and lobar renal veins). The initial step of the VExUS protocol estimates the right atrial pressure (RAP) through M-mode US of the inferior vena cava (IVC), with a cut-off point of 2 cm for the maximum anteroposterior diameter of the IVC to indicate an elevated RAP. During clinical practice, the IVC maximum diameter is manually determined with the annotation tool available on the device, thus being a highly observer-dependent task. As an alternative to improve reproducibility, in this work we present an automated segmentation method for the measurement of the maximum diameter of the IVC from M-mode ultrasound (US) images.

2. Materials

For the development and validation of the proposed system, we collected 20 images from 13 CRS patients admitted to the Internal Medicine Department of the Hospital Clínico Universitario "Lozano Blesa" in Zaragoza (Spain) with a diagnosis of acute HF or uncompensated chronic HF. Between 1 and 3 images were recorded for each patient, corresponding to some or all of the hospitalization stages (admission, control and discharge). Images were acquired using a Philips Lumify portable US scanner with abdominal probe and exported in DICOM format.

3. Methods

The images were read using a custom open-source Python package [1] and were subsequently processed as follows (Fig. 1).

3.1. Preprocessing

Starting from the initial image (Fig. 2a), histogram equalization was performed to maximize contrast without losing structural information. A bilateral filter [11] was then applied in order to reduce noise while preserving edges. Let $\mathbf{I}$ be the equalized gray-scale image, S the set of possible positions in the image and $\mathbf{p}, \mathbf{q}$ actual pixel positions, the bilateral filter was defined as:

$$BF[\mathbf{I}]_{\mathbf{p}} = \frac{1}{W_p} \sum_{\mathbf{q} \in \mathbf{S}} G_{\sigma_s}(\| \mathbf{p} - \mathbf{q} \|) \mathbf{G}_{\sigma_\mathbf{r}}(\mathbf{I_p} - \mathbf{I_q}) \mathbf{I_q}, \quad (1)$$

where G_σ denotes a two-dimensional Gaussian filter and W_p is a normalization factor. The region S (kernel size) was defined as a square region of size $l \times l$, where:

$$l = \left\lfloor \frac{\lfloor \sqrt{n^2 + m^2} \cdot 0.02 \rceil}{\sqrt{2}} \right\rceil, \quad (2)$$

where n and m are the number of pixels on the vertical and horizontal axis of the image, respectively. The values of σ_s and σ_r were obtained as:

$$\sigma_s = \left\lfloor \frac{l}{2} \right\rfloor \sigma_r = \lfloor 0.35 \cdot \sigma_\mathbf{I} \rceil, \quad (3)$$

where $\sigma_\mathbf{I}$ represents the variance of $\mathbf{I}$.

The smoothed images were binarized using Otsu's method [12]. Next, a morphological opening operation was applied using a 3×3 cross-shaped structural element, followed by a closing operation using a 5×1 structural element to ensure continuity of the objects in the horizontal axis, i.e., the direction of the IVC on M-mode US images.

Finally, the edges of the resulting image (Fig. 2b) were extracted by subtracting an eroded version from the binary mask using a 3×3 cross-shaped structural element and multiplying the result by the gradient in the vertical axis. This allowed us to define intensity changes (edges) from black to white (anterior wall of the IVC) with a positive value and changes from white to black (posterior wall of the IVC) with a negative value.

[1] https://zenodo.org/records/12749178

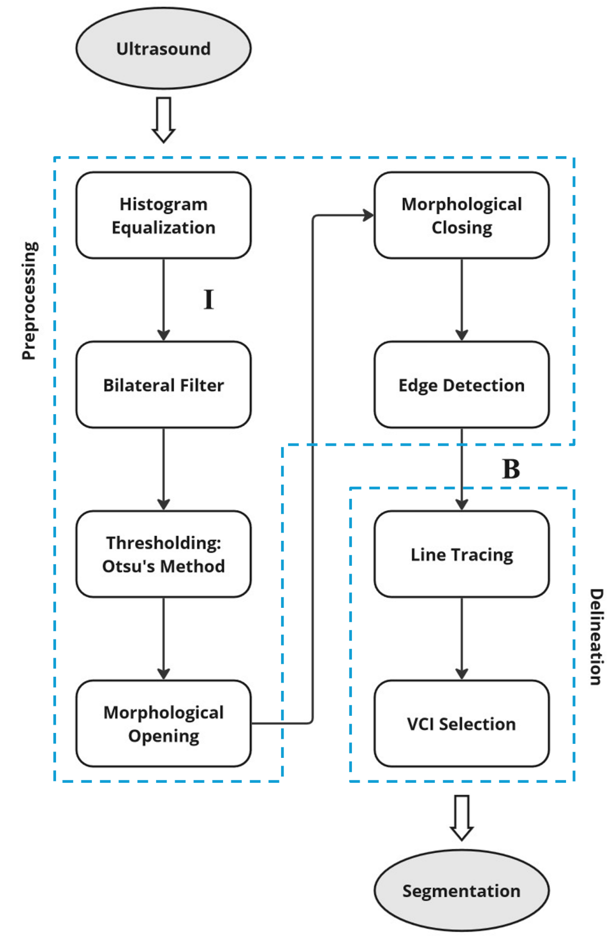

Figure 1. Proposed segmentation scheme.

3.2. Delineation

The proposed algorithm aims to identify the candidate lines for the VCI wall, pixel wise, from the images obtained in the previous step. Let $\mathbf{B}$ be a matrix of size $n \times m, \ni n, m \in N$, where each pixel is identified by the coordinates $x, y \in N \ni x = \{0, \dots, m\}, y = \{0, \dots, n\}$, and representing the edges identified with their sign of the binarized image. Let then $\mathbf{b}_j = [b_{j,0}, b_{j,1}, \dots, b_{j,n}]^T, j \in N \ni 0 \leq j \leq m$, the column vector representing the j-th column of the matrix $\mathbf{B}$. Starting at column $j = 0$ and with an empty set of identified rows, $l_1 = \phi$, the steps to identify candidate lines are as follows:

1. The coordinates of the rows, y_i, that verify that the element $b_{j,y_i} \neq 0, i \in N \ni 0 \leq i \leq n$ were identified. Each pair of coordinates $(0, y_i)$ represents the initial pixel of a candidate line l_{c_i}.
2. For each l_{c_i}, locate the coordinates of the rows, y_a, with $a = \{y_i - r, \dots, y_i + r\}$,$a, r \in N$, which verify that $sign(b_{j+1,y_a}) = sign(b_{j,y_i}), a = argmin(|y_i - y_a|)$, and

$r = 5$. This process was repeated for each value of j until no y_a was found to satisfy the condition, or $j = m + 1$ (end of image).
3. Candidate lines l_{c_i} with a length greater than 50% of the horizontal size of the image were added to the set of identified lines l_1.

This process was also performed with the image flipped on the horizontal axis, resulting in a set of lines, l_2, from right to left. Therefore, the final candidate line set was constructed as:

$$l = l_1 \cup l_2 \tag{4}$$

The set l was reordered in ascending order, with the y-coordinate of the row at the starting point of each line serving as the index for the ordering. Redundant lines were then eliminated.

Finally, let $u \in N$ be the number of lines found and $(0, y_p)$, $p \in N \ni 0 \leq p \leq u$, the coordinates of the initial pixels of the line l_p within the ordered set l, the pair of lines that verified that $positive = sign(b_{0,y_p}) \neq sign(b_{0,y_{p+1}}) = negative$ was located. This pair of lines (l_p, l_{p+1}) represents the segmentation of the VCI (Figure 2c).

3.3. Measurement extraction

From the segmentation, the distance in pixels between the VCI walls (top and bottom) was computed for all possible time instants. These values were multiplied by the spatial resolution of the image to obtain the width profile of the segmentation (Fig. 2d).

Additionally, a smoothed version of this profile was extracted with a moving average filter of length:

$$w = \left\lfloor \frac{t_d \cdot 0.05}{\Delta_x} \right\rceil \tag{5}$$

where t_d represents the duration of the data, and Δ_x is the temporal resolution of the image.

The maximum distance present in the width profile (whether smoothed or unsmoothed) is considered the maximum diameter of the IVC.

3.4. Evaluation

The maximum IVC diameters obtained with automatic segmentation (whether from smoothed or unsmoothed profiles) were compared with the maximum IVC diameter measurements obtained during clinical practice. The resulting error was expressed as mean ± standard deviation (SD). Spearman's correlation, ρ_s, and Lin's coefficient of concordance, ρ_c, were used to quantify the degree of correspondence between measurements.

Table 1. Mean error ± SD, Spearman's correlation, rho_s, and Lin's concordance coefficient, rho_c, between clinical measurements and maximum diameters of the IVC profile, smoothed and unsmoothed.

	Error (cm)	ρ_s	ρ_c
Unsmoothed	-0.015 ± 0.318	0.850	0.864
Smoothed	0.082 ± 0.291	0.879	0.879

4. Results

The available images have a temporal (horizontal) resolution of 0.003 ± 0.001 s/pixel and a spatial (vertical) resolution of 0.040 ± 0.006 cm/pixel. The resulting error and correlations values are shown in Table 1.

The average processing time was 0.235 ± 0.034 s/image on a Windows 11 PC, using an Intel Core i5-10210U 2.11 GHz processor and 16 GB RAM.

5. Discussion

This work presents an automatic segmentation method to calculate the IVC maximum diameter in M-mode US images as part of the VExUS protocol. Currently, this measurement is performed manually in clinical practice and its accuracy depends on the US measurement tools and the experience of the physician.

The error produced by the automatic method using the unsmoothed width profile is smaller than the average spatial resolution in the vertical dimension, staying below the pixel height (see Table 1). While applying the smoothed version reduces the standard deviation of the error, it introduces a larger bias of approximately two pixels. However, the smoothed version improves both Spearman's correlation and Lin's coefficient. The mean processing time is compatible with the potential integration of the algorithm into a real-time clinical tool.

The main limitation of this study is the small number of available images. Aside from that, obtaining the maximum diameter of the IVC in clinical practice is not free of error and therefore should not be considered as *gold standard* for determining the accuracy of IVC segmentation algorithms. A more accurate assessment would require manual annotations by experts. These aspects will be addressed in future extensions of this work.

6. Conclusions

The proposed method accurately identifies and segments the IVC, enabling the calculation of the maximum diameter with precision beyond the available spatial resolution. Results show a strong correlation with clinical measurements, suggesting its potential as a reliable tool for charac-

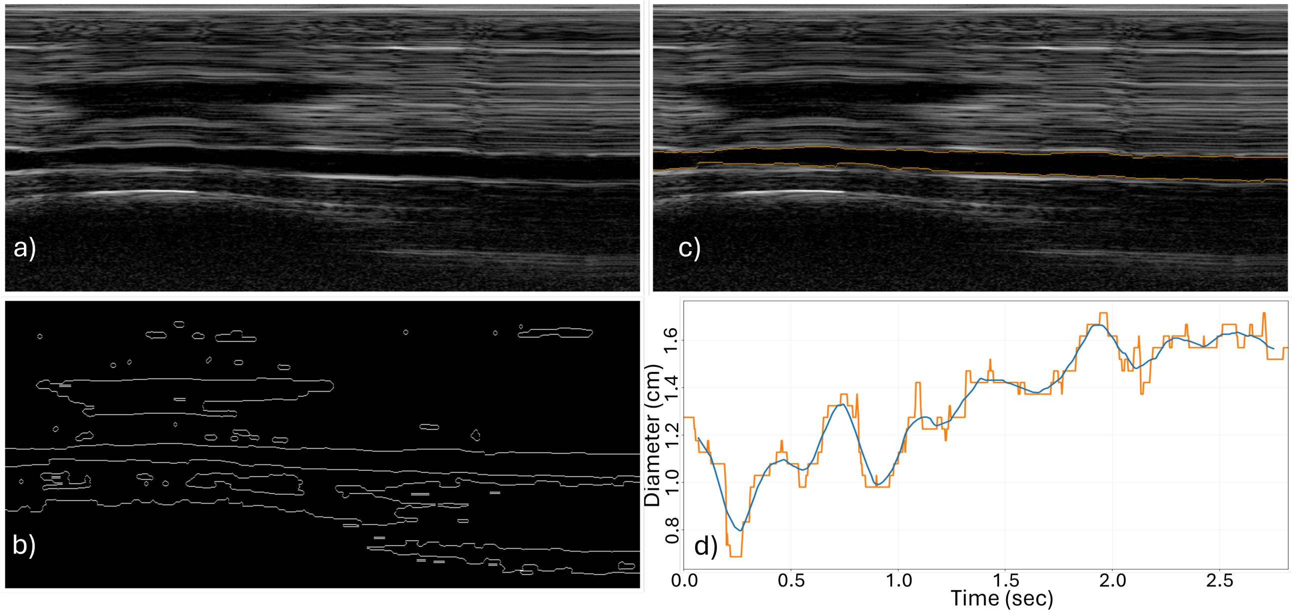

Figure 2. Segmentation steps and measurement extraction: a) M-mode US image, b) edge detection, c) IVC segmentation, d) width profiles, unsmoothed (orange trace) and smoothed (blue trace).

terizing the SVC in patients with CRS within the context of the VExUS protocol.

Acknowledgments

This work was partially funded by Departamento de Ciencia, Universidad y Sociedad del Conocimiento from Gobierno de Aragón (Spain) (Research Groups B07_23R, T39_23R and T71_23D), and by Project PID2022-139143OA-I00 funded by MICIU/AEI/10.13039/50110001 1033 and by ERDF/EU.

References

[1] World Health Organization. https://www.who.int/news-room/fact-sheets/detail/cardiovascular-diseases-(cvds). (Last accessed: July 2024).

[2] Farmakis D, Parissis J, Lekakis J, Filippatos G. Acute heart failure: Epidemiology, risk factors, and prevention. Rev Esp Cardiol March 2015;68(3):245–248.

[3] Ronco C, Haapio M, House AA, et al. Cardiorenal syndrome. J Am Coll Cardiol November 2008;52(19):1527–1539.

[4] Samoni S, Husain-Syed F, De Rosa S, Ronco C. Cardio-pulmonary-renal interactions. G Ital Nefrol March 2017; 34(69):162–177.

[5] Kazory A, Elkayam U. Cardiorenal interactions in acute decompensated heart failure: Contemporary concepts facing emerging controversies. J Card Fail December 2014; 20(12):1004–1011.

[6] Gnanaraj JF, Von Haehling S, Anker SD, et al. The relevance of congestion in the cardio-renal syndrome. Kidney Int March 2013;83(3):384–391.

[7] Rubio-Gracia J, Demissei BG, ter Maaten JM, et al. Prevalence, predictors and clinical outcome of residual congestion in acute decompensated heart failure. Int J Cardiol May 2018;258:185–191.

[8] Morrow DA, Velazquez EJ, Devore AD, et al. Clinical outcomes in patients with acute decompensated heart failure randomly assigned to sacubitril/valsartan or enalapril in the pioneer-hf trial. Circulation May 2019;139(19):2285–2288.

[9] Beaubien-Souligny W, Rola P, Haycock K, et al. Quantifying systemic congestion with point-of-care ultrasound: development of the venous excess ultrasound grading system. Ultrasound J December 2020;12(1):12–16.

[10] Rola P, Miralles-Aguiar F, Argaiz E, et al. Clinical applications of the venous excess ultrasound (vexus) score: conceptual review and case series. Ultrasound J December 2021;13(1):13–32.

[11] Tomasi C, Manduchi R. Bilateral filtering for gray and color images. In Sixth International Conference on Computer Vision. Bombay, 07 January 1998; 839–846.

[12] Otsu N. A threshold selection method from gray-level histograms. IEEE Trans Syst Man Cybern January 1979; 9(1):62–66.

Address for correspondence:

David Chaparro Victoria
E-mail: dchaparro@usj.es, Universidad San Jorge
Campus Universitario Villanueva de Gállego, Autovía A-23, Km 299, 50830, Villanueva de Gállego, Zaragoza